A Robust and Scalable Approach to Face Identification

William Robson Schwartz, Huimin Guo, and Larry S. Davis

University of Maryland, A.V. Williams Building, College Park, MD, 20742
{schwartz,hmguo,lsd}@cs.umd.edu

Abstract. The problem of face identification has received significant attention over the years. For a given probe face, the goal of face identification is to match this unknown face against a gallery of known people. Due to the availability of large amounts of data acquired in a variety of conditions, techniques that are both robust to uncontrolled acquisition conditions and scalable to large gallery sizes, which may need to be incrementally built, are challenges. In this work we tackle both problems. Initially, we propose a novel approach to robust face identification based on Partial Least Squares (PLS) to perform multi-channel feature weighting. Then, we extend the method to a tree-based discriminative structure aiming at reducing the time required to evaluate novel probe samples. The method is evaluated through experiments on FERET and FRGC datasets. In most of the comparisons our method outperforms state-of-art face identification techniques. Furthermore, our method presents scalability to large datasets.

Keywords: Face Identification, Feature combination, Feature selection, Partial Least Squares.

1 Introduction

The three primary face recognition tasks are *verification*, *identification*, and *watch list* [1]. In verification, the task is to accept or deny the identity claimed by a person. In identification, an image of an unknown person is matched to a gallery of known people. In the watch list task, a face recognition system must first detect if an individual is on the watch list. If the individual is on the watch list, the system must then correctly identify the individual. The method described in this paper addresses the identification task.

Previous research has shown that face recognition under well controlled acquisition conditions is relatively mature and provides high recognition rates even when a large number of subjects is in the gallery [2,3]. However, when images are collected under uncontrolled conditions, such as uncontrolled lighting and changes in facial expressions, the recognition rates decrease significantly.

Due to the large size of realistic galleries, not only the accuracy but also the scalability of a face identification system needs to be considered. The main scalability issues are the following. First, the number of subjects in the gallery can be

K. Daniilidis, P. Maragos, N. Paragios (Eds.): ECCV 2010, Part VI, LNCS 6316, pp. 476–489, 2010.

quite large, so that common search techniques, such as brute force nearest neighbor, employed to match probe faces do not scale well. Second, in applications such as surveillance and human computer interaction, in which new subjects are added incrementally, the necessity of rebuilding the gallery models every time a new subject is added compromises the computational performance of the system.

We tackle both problems. In order to reduce the problems associated with data collected under uncontrolled conditions, we consider a combination of low-level feature descriptors based on different clues (such approaches have provided significant improvements in object detection [4,5] and recognition [6]). Then, feature weighting is performed by Partial Least Squares (PLS), which handles very high-dimensional data presenting multicollinearity and works well even when very few samples are available [5,7,8,9]. Finally, a one-against-all classification scheme is used to model the subjects in the gallery.

To make the method scalable to the gallery size, we modify the one-against-all approach to use a tree-based structure. At each internal node of the tree, a binary classifier based on PLS regression is used to guide the search for the matching subject in the gallery. The use of this structure provides substantial reduction in the number of comparisons when a probe sample is matched against the gallery and also eliminates the need for rebuilding all PLS models when new subjects are added to the gallery.

Our proposed face identification approach outperforms state-of-art techniques in most of the comparisons considering standard face recognition datasets, particularly when the data is acquired under uncontrolled conditions, such as in experiment 4 of the FRGC dataset. In addition, our approach can also handle the problem of insufficient training data – results show high performance when only a single sample per subject is available. Finally, due to the incorporation of the tree-based structure, a significant number of comparisons can be saved when compared to approaches based on brute force nearest neighbor search.

2 Related Work

Detailed discussion of face recognition and processing can be found in recent and comprehensive surveys written by Tolba et al. [2] and Zhao et al. [3].

Most approaches to face recognition can be divided into two categories: holistic matching methods and local matching methods [10]. Methods in the former category use the whole face region to perform recognition and includes techniques such as subspace discriminant analysis, SVM, and AdaBoost; these may not cope well with the generalizability problem due to the unpredictable distribution of real-world testing face images. Methods in the latter category first locate several facial features and then classify the faces according to local statistics.

Local binary patterns (LBP) and Gabor filters are descriptors widely used in face recognition. LBP is robust to illumination variations due to its invariance to monotonic gray-scale changes and Gabor filters are also robust to illumination variations since they detect amplitude-invariant spatial frequencies of pixel gray values [10]. There are several combinations or variations based on these descriptors that have been used for face recognition [6,11,12,13].

Most recently developed face recognition systems work well when images are obtained under controlled conditions or when the test image is captured under similar conditions to those for the training images. However, under varying lighting or aging effects, their performance is still not satisfactory. To perform recognition under fairly uncontrolled conditions Tan and Triggs [14] proposed a preprocessing chain for illumination normalization. They used the local ternary patterns and a Hausdorff-like distance measure. Holappa [15] used local binary pattern texture features and proposed a filter optimization procedure for illumination normalization. Aggarwal [16] presented a physical model using Lambert's Law to generalize across varying situations. Shih [17] proposed a new color space LC_1C_2 as a linear transformation of the RGB color space.

Another challenge is that most current face recognition algorithms perform well when several training images are available per subject; however they are still not adequate for scenarios where a single sample per subject is available. In real world applications, one training sample per subject presents advantages such as ease of collect galleries, low cost for storage and lower computational cost [18]. Thus, a robust face recognition system able to work with both single and several samples per subject is desirable. In [19], Liu et al. proposed representing each single (training, testing) image as a subspace spanned by synthesized shifted images and designed a new subspace distance metric.

Regarding the scalability issues discussed previously, there is also previous work focused on scaling recognition systems to large datasets. In [20] a technique for combining rejection classifiers into a cascade is proposed to speed up the nearest neighbor search for face identification. Guo and Zhang [21] proposed the use of a constrained majority voting scheme for AdaBoost to reduce the number of comparisons needed.

3 Proposed Method

In this section, we first present the feature extraction process and a brief review of partial least squares regression. Then, the proposed face identification approach is explained in two steps. Initially, we describe the one-against-all approach, then we describe the tree-based structure, which improves scalability when the gallery is large and reduces the computational cost of matching probe samples.

3.1 Feature Extraction

After cropping and resizing the faces, each sample is decomposed into overlapping blocks and a set of low-level feature descriptors is extracted from each block. The features used include information related to shape (histogram of oriented gradients (HOG) [22]), texture (captured by local binary patterns (LBP) [13]), and color information (captured by averaging the intensities of pixels in a block).

HOG captures edge or gradient structures that are characteristic of local shape [22]. Since the histograms are computed for regions of a given size, HOG is robust to some location variability of face parts. HOG is also invariant to rotations smaller than the orientation bin size.

Local binary patterns [13] have been successfully applied in texture classification. LBP's characterize the spatial structure of the local image texture and are invariant under monotonic transformations of the pixel gray values. The LBP operator labels the pixels of an image by thresholding the 3×3 neighborhood of each pixel using the center value. A label is obtained by multiplication of the thresholded values by the binomial factors 2^p followed by their addition. The 256-bin histogram of the resulting labels is used as a feature descriptor.

Once the feature extraction process is performed for all blocks inside a cropped face, features are concatenated creating a high-dimensional feature vector $\boldsymbol{v}$. This vector is used to describe the face.

3.2 Partial Least Squares Regression

Partial least squares is a method for modeling relations between sets of observed variables by means of latent variables. PLS estimates new predictor variables, latent variables, as linear combinations of the original variables summarized in a matrix $\boldsymbol{X}$ of predictor variables (features) and a vector $\boldsymbol{y}$ of response variables. Detailed descriptions of the PLS method can be found in [23,24].

Let $\mathcal{X} \subset \mathbb{R}^m$ denote an m-dimensional feature space and let $\mathcal{Y} \subset \mathbb{R}$ be a 1-dimensional space of responses. Let the number of samples be n. PLS decomposes matrix $\boldsymbol{X}_{n \times m} \in \mathcal{X}$ and vector $\boldsymbol{y}_{n \times 1} \in \mathcal{Y}$ into

$$\boldsymbol{X} = \boldsymbol{T}\boldsymbol{P}^T + \boldsymbol{E}$$
$$\boldsymbol{y} = \boldsymbol{U}\boldsymbol{q}^T + \boldsymbol{f}$$

where $\boldsymbol{T}$ and $\boldsymbol{U}$ are $n \times p$ matrices containing p extracted latent vectors, the $(m \times p)$ matrix $\boldsymbol{P}$ and the $(1 \times p)$ vector $\boldsymbol{q}$ represent the loadings and the $n \times m$ matrix $\boldsymbol{E}$ and the $n \times 1$ vector $\boldsymbol{f}$ are the residuals. Using the nonlinear iterative partial least squares (NIPALS) algorithm [7], a set of weight vectors is constructed, stored in the matrix $\boldsymbol{W} = (\boldsymbol{w}_1, \boldsymbol{w}_2, \ldots, \boldsymbol{w}_p)$, such that

$$[cov(\boldsymbol{t}_i, \boldsymbol{u}_i)]^2 = \max_{|\boldsymbol{w}_i|=1} [cov(\boldsymbol{X}\boldsymbol{w}_i, \boldsymbol{y})]^2 \tag{1}$$

where $\boldsymbol{t}_i$ is the i-th column of matrix $\boldsymbol{T}$, $\boldsymbol{u}_i$ the i-th column of matrix $\boldsymbol{U}$ and $cov(\boldsymbol{t}_i, \boldsymbol{u}_i)$ is the sample covariance between latent vectors $\boldsymbol{t}_i$ and $\boldsymbol{u}_i$. After extracting the latent vectors $\boldsymbol{t}_i$ and $\boldsymbol{u}_i$, the matrix $\boldsymbol{X}$ and vector $\boldsymbol{y}$ are deflated by subtracting their rank-one approximations based on $\boldsymbol{t}_i$ and $\boldsymbol{u}_i$. This process is repeated until the desired number of latent vectors has been extracted.

Once the low dimensional representation of the data has been obtained by NIPALS, the regression coefficients $\boldsymbol{\beta}_{m \times 1}$ can estimated by

$$\boldsymbol{\beta} = \boldsymbol{W}(\boldsymbol{P}^T\boldsymbol{W})^{-1}\boldsymbol{T}^T\boldsymbol{y}. \tag{2}$$

The regression response, y_v, for a feature vector $\boldsymbol{v}$ is obtained by

$$y_v = \overline{y} + \boldsymbol{\beta}^T\boldsymbol{v} \tag{3}$$

where $\overline{y}$ is the sample mean of $\boldsymbol{y}$.

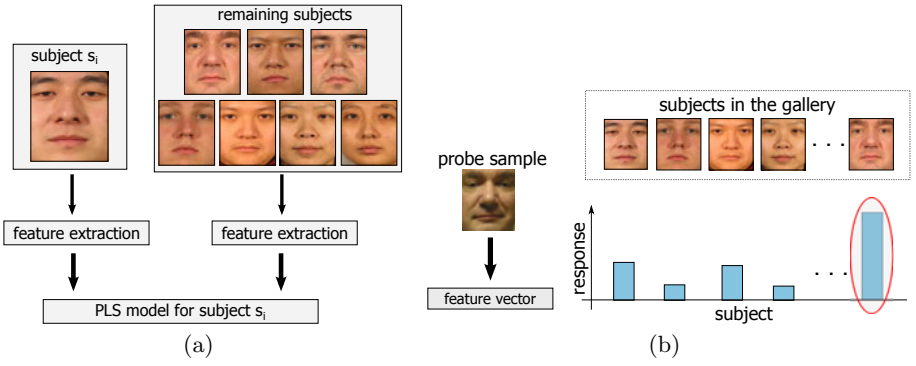

Fig. 1. One-against-all face identification approach. (a) construction of the PLS regression model for a subject in the gallery; (b) matching of a probe sample against the subjects in the gallery. The best match for a given probe sample is the one associated with the PLS model presenting the highest regression response.

Notice that even though the number of latent vectors used to create the low dimensional representation of the data matrix $\boldsymbol{X}$ is p (possibly greater than 1), Equation 3 shows that only a single dot product of a feature vector with the regression coefficients is needed to obtain the response of a PLS regression model – and it is this response that is used to rank faces in a gallery. This characteristic makes the use of PLS particularly fast for finding matches for novel probe samples, in contrast to other methods where the number of dot product evaluations depends on the number of eigenvectors considered, which is quite large in general [25].

3.3 One-Against-All Approach

The procedure to learn models for subjects in the gallery $g = \{\boldsymbol{s}_1, \boldsymbol{s}_2, \ldots, \boldsymbol{s}_n\}$, where $\boldsymbol{s}_i$ represents exemplars of each subject's face, is illustrated in Figure 1(a) and described in details as follows. Each $\boldsymbol{s}_i$ is composed of feature vectors extracted from cropped faces containing examples of the i-th subject.

We employ a one-against-all scheme to learn a PLS discriminatory model for each subject in the gallery. Therefore, when the i-th subject is considered, the remaining samples $g \setminus \boldsymbol{s}_i$ are used as counter-examples of the i-th subject. In addition, if the face dataset provides a training set we also add those samples, (excluding samples from the subject under consideration), as counter-examples of the i-th subject. Experiments show that the addition of training samples as counter-examples improves recognition rates.

When a one-against-all scheme is used with PLS, higher weights are attributed to features located in regions containing discriminatory characteristics between the subject under consideration and the remaining subjects.

Once the models have been estimated for all subjects in the gallery, the PLS regression models are stored to be later used to evaluate the responses for a probe

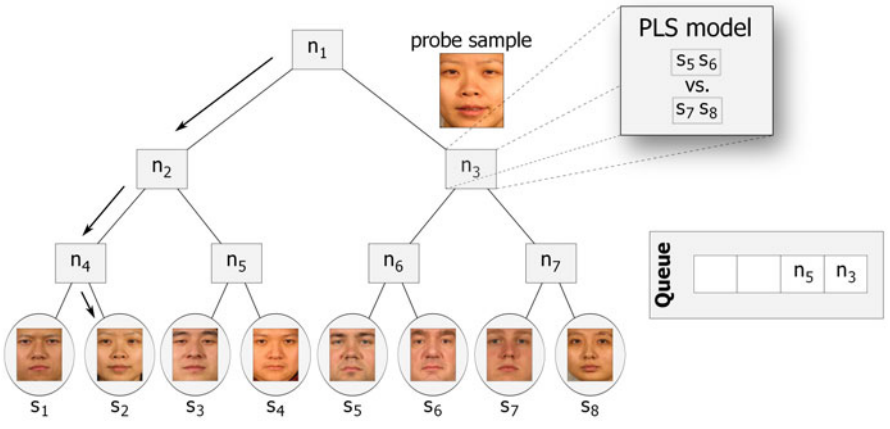

Fig. 2. Tree-based structure used to optimize the search for matches to a probe sample. Each internal node contains a PLS regression model used to guide the search, as shown in details for node n_3, which has a PLS model constructed so that the response directs the search either to node n_6 or n_7. In this example the first path to be traversed is indicated by arrows (in this case, it leads to the correct match for this particular probe sample). Alternative search paths are obtained by adding nodes that have not been visited into a priority queue (in this example nodes n_3 and n_5 will be the starting nodes for additional search paths). After pursuing a number of search paths leading to different leaf nodes, the best match is chosen to be the one presenting the highest response (in absolute value).

sample. Then, when a probe sample is presented, its feature vector is projected onto each one of the PLS models. The model presenting the highest regression response gives the best match for the probe sample, as illustrated in Figure 1(b).

3.4 Optimization Using a Tree-Based Structure

In terms of scalability, two drawbacks are present in the one-against-all scheme described in the previous section. First, when a new subject is added to the gallery, PLS models need to be rebuilt for all subjects. Second, to find the best match to a probe sample, the feature vector representing this sample needs to be projected onto all PLS models learned for the subjects in the gallery (common problem faced by methods that estimate matching scores using brute force nearest neighbor search [20]).

To reduce the need for projecting features onto all PLS models to find the best match for a probe sample, we construct a binary tree in which each node, n_j, contains a subset of the gallery subjects $t_j \subset g$, where $g = \{\boldsymbol{s}_1, \boldsymbol{s}_2, \ldots, \boldsymbol{s}_n\}$ as defined previously. A splitting procedure is used to decide which elements of t_j will belong to the left and right children of n_j, assigning at least one sample to each child. Each internal node is associated with a PLS regression model, used afterwards to guide the search when probe samples are analyzed. In order

to build the regression model for a node, the subjects assigned to the left child are defined to have response -1 and the subjects assigned to the right child are defined to have response $+1$. The splitting procedure and the building of PLS models are applied recursively in the tree until a node contains only a single subject (leaf node).

The application of the described procedure for a gallery with n subjects results in a tree containing n leaf nodes and $n-1$ PLS regression models located on the internal nodes.

We consider two approaches to split subjects between the children nodes. First, a procedure that uses PCA to create a low dimensional subspace (learned using samples from a training set) and then the K-means algorithm clusters data into two groups, each one is assigned to one child. The second approach chooses random splits and divides the subjects equally into two groups. We evaluate these splitting procedures in Section 4.3.

When a feature vector describing a probe sample is analyzed to find its best matching subject in the gallery, a search starting from the root of the tree is performed. At each internal node, the feature vector is projected onto the PLS model and according to its response, the search continues either from the left or from the right child. The search stops when a leaf node is reached. Figure 2 illustrates this procedure.

According to experimental results shown in Section 4.3, the traversal of a few search paths is enough to obtain the best match for a probe sample. Starting nodes for alternative search paths are stored in a priority queue. An internal node n_k is pushed into the priority queue when its sibling is chosen to be in the current search path. The priority associated with n_k is proportional to its response returned by the PLS regression model at its parent. Finally, since each search path leads to a leaf node, the best match for a given probe sample is chosen to be the one presenting the highest response (in absolute value) among the leaf nodes reached during the search.

The tree-based structure can also be used to avoid rebuilding all PLS models when a new subject is added into the gallery. Assuming that a tree is built for k subjects, the procedure to add a new subject $\boldsymbol{s}_{k+1}$ is described as follows. Choose a leaf node n_i, where $t_i = \{\boldsymbol{s}_j\}$; set n_i to be an internal node and create two new leaf nodes to store $\boldsymbol{s}_j$ and $\boldsymbol{s}_{k+1}$; then, build a PLS model for node n_i (now with $t_i = \{\boldsymbol{s}_j, \boldsymbol{s}_{k+1}\}$). Finally, rebuild all PLS models in nodes having n_i as a descendant. Therefore, using this procedure, the number of PLS models that needs to be rebuilt when a new subject is added no longer depends on the number of subjects in the gallery, but only on the depth of node n_i.

4 Experiments

In this section we evaluate several aspects of our proposed approach. Initially, we show that the use of the low-level feature descriptors analyzed by PLS in a one-against-all scheme, as described in Section 3.3, improves recognition rates over previous approaches, particularly when the data is acquired under uncontrolled

conditions. Then, we demonstrate that the tree-based approach introduced in Section 3.4 obtains comparably high recognition rates with a significant reduction in the number of projections.

The method is evaluated on two standard datasets used for face recognition: FERET and FRGC version 1. The main characteristics of the FERET dataset are that it contains a large number of subjects in the gallery and the probe sets exploit differences in illumination, facial expression variations, and aging effects [26]. FRGC contains faces acquired under uncontrolled conditions [27].

All experiments were conducted on an Intel Core i7-860 processor, 2.8 GHz with 4GB of RAM running Windows 7 operating system using a single processor core. The method was implemented using C++ programming language.

4.1 Evaluation on the FERET Dataset

The frontal faces in the FERET database are divided into five sets: fa (1196 images, used as gallery set containing one image per person), fb (1195 images, taken with different expressions), fc (194 images, taken under different lighting conditions), $dup1$ (722 images, taken at a later date), and $dup2$ (234 images, taken at least one year apart). Among these four standard probe sets, $dup1$ and $dup2$ are considered the most difficult since they are taken with time-gaps, so some facial features have changed. The images are cropped and rescaled to 110×110 pixels.

Experimental Setup. Since the FERET dataset is taken under varying illumination conditions, we preprocessed the images for illumination normalization. Among the best known illumination normalization methods are the self-quotient image (SQI) [28], total variation models, and anisotropic smoothing [15]. SQI is a retinex-based method which does not require training images and has relatively low computational complexity; we use it due to its simplicity. Once the images are normalized, we perform feature extraction. For HOG features we use block sizes of 16×16 and 32×32 with strides of 4 and 8 pixels, respectively. For LBP features we use block size of 32×32 with a stride of 16 pixels. The mean features are computed from block size of 4×4 with stride of 2 pixels. This results in feature vectors with $35,680$ dimensions.

To evaluate how the method performs using information extracted exclusively from a single image per subject, in this experiment we do not add samples from the training set as counter-examples. The training set is commonly used to build a subspace to obtain a low dimensional representation of the features before performing the match. This subspace provides additional information regarding the domain of the problem.

Results and Comparisons. Figure 3(a) shows the cumulative match curves obtained by the one-against-all approach for all FERET probe sets. We see that our method is robust to facial expressions (fb), lighting (fc) and aging effect ($dup1$, $dup2$). The computational time to learn the gallery models is 4519 s and the average time to evaluate a pair of probe-gallery samples is 0.34 ms.

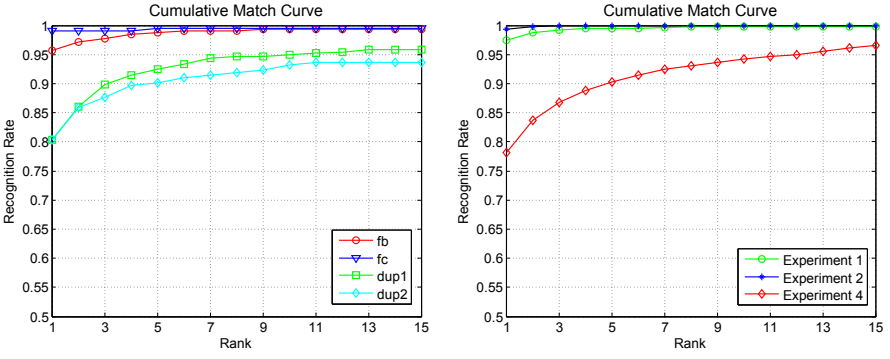

(a) FERET (b) FRGC

Fig. 3. The cumulative match curve for the top 15 matches obtained by the one-against-all approach based on PLS regression for FERET and FRGC datasets

Table 1 shows the rank-1 recognition rates of previously published algorithms and ours on the FERET dataset. As shown in the table, the one-against-all approach achieves similar results on fb and fc without using the training set. Additionally, our results on the challenging $dup1$ and $dup2$ sets are over 80%.

Table 1. Recognition rates of the one-against-all proposed identification method compared to algorithms for the FERET probe sets

	Method	**fb**	**fc**	**dup1**	**dup2**
using training set	Best result of [26]	95.0	82.0	59.0	52.0
	LBP [13]	97.0	79.0	66.0	64.0
	Tan [6]	98.0	98.0	90.0	85.0
not using training set	LGBPHS [11]	98.0	97.0	74.0	71.0
	HGPP [12]	97.6	98.9	77.7	76.1
	SIS [19]	91.0	90.0	68.0	68.0
	Ours	95.7	99.0	80.3	80.3

4.2 Evaluation on the FRGC Dataset

We evaluate our method using three experiments of FRGC version 1 that consider 2D images. Experiment 1 contains a single controlled probe image and a gallery with one controlled still image per subject (183 training images, 152 gallery images, and 608 probe images). Experiment 2 considers identification of a person given a gallery with four controlled still images per subject (732 training images, 608 gallery images, and 2432 probe images). Finally, experiment 4 considers a single uncontrolled probe image and a gallery with one controlled still image per subject (366 training images, 152 gallery images, and 608 probe

Table 2. Recognition rates of the one-against-all proposed identification method compared to other algorithms for the FRGC probe sets

Method	**Exp.1**	**Exp.2**	**Exp.4**
UMD [16]	94.2	99.3	-
LC_1C_2 [17]	-	-	75.0
Tan (from [15])	-	-	58.1
Holappa [15]	-	-	63.7
Ours	97.5	99.4	78.2

images). We strictly followed the published protocols. The images are cropped and rescaled to 275×320 pixels.

Experimental Setup. FRGC images are larger than FERET; thus we have chosen larger block sizes and strides to avoid computing too many features. For HOG features we use block sizes of 32×32 with strides of 8 pixels. For LBP features we use block size of 32×32 with strides of 24 pixels. And the mean features are extracted from block sizes of 8×8 with a stride of 4 pixels. This results in feature vectors with $86,634$ dimensions.

Experiment 4 in FRGC version 1 is considered the most challenging in this dataset. Since it is hard to recognize uncontrolled faces directly from the gallery set consisting of controlled images, we attempted to make additional use of the training set to create some *uncontrolled environment information* using morphed images. Morphing can generate images with reduced resemblance to the imaged person or look-alikes of the imaged person [29]. The idea is to first compute a *mean face* from the uncontrolled images in the training set. Then, we perform triangulation-based morphing from the original gallery set to this mean face by 20%, 30%, 40%. This generates three synthesized images. Therefore, for each subject in the gallery we now have four samples.

Results and Comparisons. Figure 3(b) shows the cumulative match curves obtained by the one-against-all approach for the three probe sets of FRGC. In addition, the computational time to learn gallery models is 410.28 s for experiment 1, 1514.14 s for experiment 2, and 1114.39 s for experiment 4. The average time to evaluate a pair of probe-gallery samples is 0.61 ms.

Table 2 shows the rank-1 recognition rates of different algorithms on the FRGC probe sets. Our method outperforms others in every probe set considered, especially on the most challenging experiment 4. This is, to the best of our knowledge, the best performance reported in the literature.

4.3 Evaluation of the Tree-Based Structure

In this section we evaluate the tree-based structure described in Section 3.4. First, we evaluate procedures used to split the set of subjects belonging to a node. Second, we test heuristics used to reduce the search space. Third, we compare the

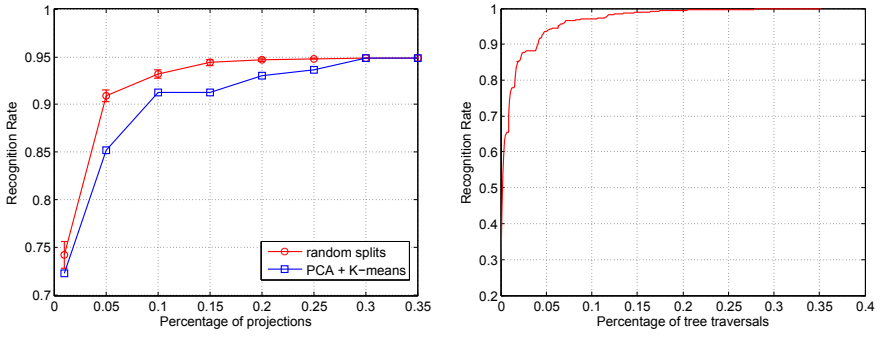

Fig. 4. Evaluation of the tree-based approach. (a) comparison of the recognition rates when random splits and PCA+K-Means approach are used; (b) evaluation of the heuristic based on stopping the search after a maximum number of tree traversals is reached.

results obtained previously by the one-against-all approach to results obtained when the tree-based structure is incorporated. Finally, we compare our method to the approach proposed by Yuan et al. [20].

To evaluate the reduction in the number of comparisons, in this section the x-axis of the plots no longer displays the rank; instead it shows either the percentage of projections performed by the tree-based approach when compared to the one-against-all approach (e.g. Figure 4(a)) or the percentage of tree traversals when compared to the number of subjects in the gallery (e.g. Figure 4(b)). The y-axis displays the recognition rates for the rank-1 matches. We used probe set *fb* from the FERET dataset to perform evaluations in this section.

Procedure to Split Nodes. Figure 4(a) shows that both splitting procedures described in Section 3.4 obtain similar recognition rates when the same number of projections is performed. The error bars (in Figure 4(a)) show the standard deviation of the recognition rates obtained using random splits. They are very low and negligible when the percentage of projections increases. Due to the similarity of the results, we have chosen to split the nodes randomly. The advantages of applying random splits are the lower computational cost to build the gallery models and balanced trees are obtained. Balanced trees are important since the depth of a leaf node is proportional to $\lg n$, which is desirable to keep short search paths.

Heuristics to Reduce the Search Space. The first experiment evaluates the recognition rate as a function of the maximum number of traversals allowed to find the match subject to a probe sample; this is limited to a percentage of the gallery size. Figure 4(b) shows the maximum recognition rates achievable for a given percentage. We can see that as low as 15% of traversals are enough to obtain recognition rates comparable to the results obtained by the one-against-all approach (95.7% for the probe set considered in this experiment).

In the second experiment we consider the following heuristic. For the initial few probe samples, all search paths are evaluated and the absolute values of the

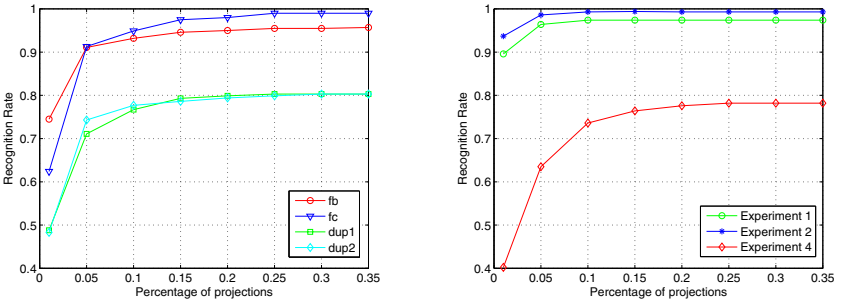

(a) FERET (b) FRGC

Fig. 5. Recognition rates as a function of the percentage of projections performed by the tree-based approach when compared to the one-against-all approach

regression responses for the best matches are stored. The median of these values is computed. Then, for the remaining probe samples, the search is stopped when the regression response for a leaf node is higher than the estimated median value. Our experiments show that this heuristic alone is able to reduce the number of projections to 63% without any degradation in the recognition rates.

Results and Comparisons. Using the results obtained from the previous experiments (random splits and adding both heuristics to reduce the search space), we now compare the recognition rates obtained when the tree-based structure is used to results obtained by the one-against-all approach. Then, we evaluate the speed-up achieved by reducing the number of projections.

Figures 5(a) and 5(b) show identification results obtained for FERET and FRGC datasets, respectively. Overall, we see that when the number of projections required by the one-against-all approach is reduced to 20% or 30%, there is a negligible drop in the recognition rate shown in the previous sections. Therefore, without decreasing the recognition rate, the use of the tree-based structure provides a clear speed-up for performing the evaluation of the probe set. According to the plots, speed-ups of 4 times are achieved for FERET, and for FRGC the speed-up is up to 10 times depending on the experiment being considered.

Finally, we compare our method to the *cascade of rejection classifiers* (CRC) approach proposed by Yuan et al. [20]. Table 3 shows the speed-ups over the

Table 3. Comparison between our tree-based approach and the CRC approach

	test set size as fraction of dataset	**10%**	**21%**	**32%**	**43%**	**65%**
CRC	speed-up	1.58	1.58	1.60	2.38	3.35
	rank-1 error rate	19.5%	22.3%	24.3%	28.7%	42.0%
Ours	speed-up	3.68	3.64	3.73	3.72	3.80
	rank-1 error rate	5.62%	5.08%	5.70%	5.54%	5.54%

brute force nearest neighbor search and rank-1 error rates obtained by both approaches. We apply the same protocol used in [20] for the FRGC dataset. Higher speed-ups are obtained by our method and, differently from CRC, no increase in the error rates is noticed when larger test set sizes are considered.

5 Conclusions

We have proposed a face identification method using a set of low-level feature descriptors analyzed by PLS which presents the advantages of being both robust and scalable. Experimental results have shown that the method works well for single image per sample, in large galleries, and under different conditions.

The use of PLS regression makes the evaluation of probe-gallery samples very fast due to the necessity of only a single dot product evaluation. Optimization is further improved by incorporating the tree-based structure, which reduces largely the number of projections when compared to the one-against-all approach, with negligible effect on recognition rates.

Acknowledgments

This research was funded by the Office of the Director of National Intelligence (ODNI), Intelligence Advanced Research Projects Activity (IARPA), through the Army Research Laboratory (ARL). All statements of fact, opinion or conclusions contained herein are those of the authors and should not be construed as representing the official views or policies of IARPA, the ODNI, or the U.S. Government.

References

1. Phillips, P.J., Micheals, P.J., Blackburn, R.J., Tabassi, D.M., Bone, J.M.: Face Recognition vendor test 2002: Evaluation Report. Technical report, NIST (2003)
2. Tolba, A., El-Baz, A., El-Harby, A.: Face recognition: A literature review. International Journal of Signal Processing 2, 88–103 (2006)
3. Zhao, W., Chellappa, R., Phillips, P.J., Rosenfeld, A.: Face recognition: A literature survey. ACM Comput. Surv. 35, 399–458 (2003)
4. Wu, B., Nevatia, R.: Optimizing discrimination-efficiency tradeoff in integrating heterogeneous local features for object detection. In: CVPR, pp. 1–8 (2008)
5. Schwartz, W.R., Kembhavi, A., Harwood, D., Davis, L.S.: Human detection using partial least squares analysis. In: ICCV (2009)
6. Tan, X., Triggs, B.: Fusing Gabor and LBP feature sets for kernel-based face recognition. In: Zhou, S.K., Zhao, W., Tang, X., Gong, S. (eds.) AMFG 2007. LNCS, vol. 4778, pp. 235–249. Springer, Heidelberg (2007)
7. Wold, H.: Partial least squares. In: Kotz, S., Johnson, N. (eds.) Encyclopedia of Statistical Sciences, vol. 6, pp. 581–591. Wiley, New York (1985)
8. Schwartz, W.R., Davis, L.S.: Learning discriminative appearance-based models using partial least squares. In: SIBGRAPI (2009)
9. Dhanjal, C., Gunn, S., Shawe-Taylor, J.: Efficient sparse kernel feature extraction based on partial least squares. TPAMI 31, 1347–1361 (2009)

10. Zou, J., Ji, Q., Nagy, G.: A comparative study of local matching approach for face recognition. IEEE Transactions on Image Processing 16, 2617–2628 (2007)
11. Zhang, W., Shan, S., Gao, W., Chen, X., Zhang, H.: Local gabor binary pattern histogram sequence (LGBPHS): A novel non-statistical model for face representation and recognition. In: ICCV 2005, pp. 786–791 (2005)
12. Zhang, B., Shan, S., Chen, X., Gao, W.: Histogram of gabor phase patterns (HGPP): A novel object representation approach for face recognition. IEEE Transactions on Image Processing 16, 57–68 (2007)
13. Ahonen, T., Hadid, A., Pietikainen, M.: Face recognition with local binary patterns. In: Pajdla, T., Matas, J(G.) (eds.) ECCV 2004. LNCS, vol. 3021, pp. 469–481. Springer, Heidelberg (2004)
14. Tan, X., Triggs, B.: Enhanced local texture feature sets for face recognition under difficult lighting conditions. In: Zhou, S.K., Zhao, W., Tang, X., Gong, S. (eds.) AMFG 2007. LNCS, vol. 4778, pp. 168–182. Springer, Heidelberg (2007)
15. Holappa, J., Ahonen, T., Pietikinen, M.: An optimized illumination normalization method for face recognition. In: IEEE International Conference on Biometrics: Theory, Applications and Systems, pp. 6–11 (2008)
16. Aggarwal, G., Biswas, S., Chellappa, R.: UMD experiments with FRGC data. In: CVPR Workshop, pp. 172–178 (2005)
17. Shih, P., Liu, C.: Evolving effective color features for improving FRGC baseline performance. In: CVPR Workshop, pp. 156–163 (2005)
18. Tan, X., Chen, S., Zhou, Z., Zhang, F.: Face recognition from a single image per person: A survey. Pattern Recognition 39, 1725–1745 (2006)
19. Liu, J., Chen, S., Zhou, Z., Tan, X.: Single image subspace for face recognition. In: Zhou, S.K., Zhao, W., Tang, X., Gong, S. (eds.) AMFG 2007. LNCS, vol. 4778, pp. 205–219. Springer, Heidelberg (2007)
20. Yuan, Q., Thangali, A., Sclaroff, S.: Face identification by a cascade of rejection classifiers. In: CVPR Workshop, pp. 152–159 (2005)
21. Guo, G.D., Zhang, H.J.: Boosting for fast face recognition. In: ICCV Workshop. IEEE Computer Society, Los Alamitos (2001)
22. Dalal, N., Triggs, B.: Histograms of Oriented Gradients for Human Detection. In: CVPR, pp. 886–893 (2005)
23. Elden, L.: Partial least-squares vs. Lanczos bidiagonalization–I: analysis of a projection method for multiple regression. Computational Statistics & Data Analysis 46, 11–31 (2004)
24. Rosipal, R., Kramer, N.: Overview and recent advances in partial least squares. In: Saunders, C., Grobelnik, M., Gunn, S., Shawe-Taylor, J. (eds.) SLSFS 2005. LNCS, vol. 3940, pp. 34–51. Springer, Heidelberg (2006)
25. Delac, K., Grgic, M., Grgic, S.: Independent comparative study of PCA, ICA, and LDA on the FERET data set. International Journal of Imaging Systems and Technology 15, 252–260 (2005)
26. Phillips, P.J., Moon, H., Rizvi, S.A., Rauss, P.J.: The FERET evaluation methodology for face-recognition algorithms. TPAMI 22, 1090–1104 (2000)
27. Phillips, P.J., Flynn, P.J., Scruggs, T., Bowyer, K.W., Chang, J., Hoffman, K., Marques, J., Min, J., Worek, W.: Overview of the face recognition grand challenge. In: CVPR, pp. 947–954 (2005)
28. Wang, H., Li, S.Z., Wang, Y.: Face recognition under varying lighting conditions using self quotient image. In: IEEE International Conference on Automatic Face and Gesture Recognition, pp. 819–824 (2004)
29. Kamgar Parsi, B., Lawson, E., Baker, P.: Toward a human-like approach to face recognition. In: BTAS, pp. 1–6 (2007)